Engineering Analysis with Boundary Elements ▮ (▮▮▮▮) ▮▮▮–▮▮▮

Contents lists available at ScienceDirect

Engineering Analysis with Boundary Elements

journal homepage: www.elsevier.com/locate/enganabound

Boundary element analysis of 2D thin walled structures with high-order geometry elements using transformation

Yao-Ming Zhang [a,*], Yan Gu [a], Jeng-Tzong Chen [b]

[a] Institute of Applied Mathematics, Shandong University of Technology, Zibo 255049, Shandong Province, China
[b] Department of Harbor and River Engineering, National Taiwan Ocean University, Keelung 20224, Taiwan

ARTICLE INFO

Article history:
Received 27 November 2009
Accepted 13 July 2010

Keywords:
Boundary element method
Nearly singular integrals
Thin bodies
Curved surface elements
Transformation
Elasticity problem

ABSTRACT

Thin structures have been widely designed and utilized in many industries. However, the analysis of the mechanical behavior of such structures represents a very challenging and attractive task to scientists and engineers because of their special geometrical shapes. The major difficulty in applying the boundary element method (BEM) to thin structures is the coinstantaneous existence of the singular and nearly singular integrals in conventional boundary integral equation (BIE). In this paper, a non-linear transformation over curved surface elements is introduced and applied to the indirect regularized boundary element method for 2-D thin structural problems. The developed transformation can remove or damp out the nearly singular properties of the integral kernels, based on the idea of diminishing the difference of the orders of magnitude or the scale of change of operational factors. For the test problems studied, very promising results are obtained when the thickness to length ratio is in the orders of 1E−01 to 1E−06, which is sufficient for modeling most thin structures in industrial applications.

1. Introduction

With the advances in material science and manufacturing, more and more thin structures are frequently used for the design in various industrial applications, such as coating or multi-coating on machine components, sensors in smart materials and various thin films in electronic devices. However, the widespread experimental research in thin structure problems underlies a general lack of modeling efforts that represents a great challenge to researchers in computational mechanics.

For computational models of thin structures or thin shapes in structures, two numerical methods can be employed: the finite element method (FEM) and the boundary element method (BEM). The FEM is a successful tool for the analysis of many industrial applications. However, the FEM element count increases dramatically for thin structures due to aspect ratio limitations, and the procedure therefore requires too much preprocessing and CPU time as the thickness decreases. It is long believed that the BEM is more efficient and accurate in thin structural problems due to the boundary-only discretizations and its semi-analytical nature [1–3]. However, the conventional boundary element method (CBEM) cannot be applied readily to thin structures, because of the nearly singular integral problem.

The nearly singular integrals are not singular in the sense of mathematics. However, from the point of view of numerical integrations, these integrals cannot be calculated accurately by using the conventional numerical quadrature since the integrand oscillates very fiercely within the integration interval. Although that difficulty can be overcome by using very fine meshes, the process requires too much preprocessing and CPU time. In the past decades, tremendous effort is devoted to derive convenient integral forms or sophisticated computational techniques for calculating the nearly singular integrals. These proposed methods include, but are not limited to, interval subdivision method [4,5], special Gaussian quadrature method [6], exact integration method [7–10], and various non-linear transformation methods [11–16]. In recent studies, the above methods have been reviewed in detail by Zhang et al. [17] and Zhang and Sun [18].

Among the above methods, the transformation deserves special mention due to the wide suitability and higher accuracy. Most of previous transformations can be generalized into two categories: one is removing the nearly zero factor by using another zero factor that is usually generated by Jacobian; the other one is converting the nearly zero factor in the denominator to be part of the numerator, which profits from the idea of the reciprocal transformation for the regularization of weakly singular integrals. Numerical tests show that the transformations based on the former idea are effective for the calculation of nearly weakly singular integrals but not satisfactory for nearly strong singular or nearly hypersingular integrals. The latter transformations, based on the idea of reciprocal transformation, can convert

* Corresponding author.
E-mail address: zymfc@163.com (Y.-M. Zhang).

0955-7997/$ - see front matter © 2010 Published by Elsevier Ltd.
doi:10.1016/j.enganabound.2010.07.008

nearly singular kernels into regular kernels, but the original regular parts would behave nearly singular after the transformations, so they are suitable only for a case when the regular part of the integrand is constant. During the existing transformations, the optimal transformations [11], the sinh transformation [13], and the exponential transform [17] are predicted to be more efficient, where the exponential transform is slightly better than the formers according to extensive numerical experiments.

With the development of the numerical techniques for calculation nearly singular integrals, considerable progress has been made in the application of the BEM to the analysis of thin walled structures in the past few years. Sladek et al. [19] have obtained amount of the original results in this field. Non-singular integral equations for thin-walled structures are proposed based on a subtraction technique and mathematical regularization. Liu et al. [2,20,21] have undertaken a lot of researches in this field. The nearly singular surface integrals are transformed into a sum of weakly singular integrals, and a non-linear coordinate transformation is developed for nearly weakly singular integrals. However, as shown in Ref. [22], only some boundary unknowns are computed in Liu's work. The physical quantities at interior points need further investigation. Zhou et al.[10,22] proposed semi-analytical or analytical integral algorithms to solve 2-D or 3-D thin body problems, and both boundary and interior unknowns are computed in their works.

Although great progresses have been achieved for each of the above methods, it should be pointed out that the geometry of the boundary element is often depicted by using linear shape functions when nearly singular integrals need to be calculated. In 2009, the author and co-workers proposed a general non-linear transformation for evaluation nearly singular integrals over curved surfaces arising in the boundary layer effect problem [17]. In a more recent study, the theory is also applied to thermal behavior analysis for thin-coated cutting tools [23].

This paper is an extension of our previous work [17] where a novel non-linear transformation method over curved surface elements was proposed and applied to treat the boundary layer effect occurring in 2D elasticity problems. Herein, the proposed transformation is extended to the indirect regularized boundary element method for thin structural problems of 2D elasticity problems. Both boundary and interior unknowns of thin structures with thickness-to-length ratios from $1E-1$ to $1E-6$, which is sufficient for modeling most thin structures in industrial applications, are well calculated by using the proposed approach. Owing to the employment of the high-order element, only a small number of elements need to be divided along the boundary, and high accuracy can be achieved without increasing more computational efforts. The algorithm derived in this paper substantially simplifies the programming and provided a general computational method for solving thin structure problems.

2. The BEM formulation for thin walled structural problems

In the following, the BEM formulation for general 2-D thin walled structures is developed. Using the BEM-based technique developed in [17,18], the formulation developed in this paper can be used to solve many thin structural problems with large aspect ratios.

In this paper, we always assume that Ω is a bounded domain in R^2, Ω^c is its open complement, and Γ denotes the boundary. $\boldsymbol{t}(\boldsymbol{x})$ and $\boldsymbol{n}(\boldsymbol{x})$ (or $\boldsymbol{t}$ and $\boldsymbol{n}$) are the unit tangent and outward normal vectors of Γ to the domain Ω at the point $\boldsymbol{x}$, respectively. For 2D elastic problems, the indirect regularized BIEs are given in [24]. Without regard to the rigid body displacement and the body forces, the non-singular BIEs can be expressed as

$$u_i(\mathbf{y}) = \int_\Gamma \phi_k(\mathbf{x}) u^*_{ik}(\mathbf{y},\mathbf{x}) d\Gamma, \quad \mathbf{y} \in \Gamma \tag{1}$$

$$\begin{aligned}\nabla u_i(\mathbf{y}) = {} & \hat{S}\frac{\phi_k(\mathbf{y})\hat{\mathbf{n}}(\mathbf{y})}{G}\left[\delta_{ik} - \frac{\hat{n}_k(\mathbf{y})\hat{n}_i(\mathbf{y})}{2(1-\nu)}\right] + \int_\Gamma [\phi_k(\mathbf{x}) - \phi_k(\mathbf{y})]\nabla u^*_{ik}(\mathbf{x},\mathbf{y}) d\Gamma_x \\ & - \phi_k(\mathbf{y})\left\{\int_\Gamma \left[\hat{\mathbf{t}}(\mathbf{x}) - \hat{\mathbf{t}}(\mathbf{y})\right]\frac{\partial u^*_{ik}(\mathbf{x},\mathbf{y})}{\partial \hat{\mathbf{t}}} d\Gamma_x + \int_\Gamma [\hat{\mathbf{n}}(\mathbf{x}) - \hat{\mathbf{n}}(\mathbf{y})]\frac{\partial u^*_{ik}(\mathbf{x},\mathbf{y})}{\partial \hat{\mathbf{n}}} d\Gamma_x \right. \\ & + \frac{k_0\hat{\mathbf{n}}(\mathbf{y})}{G}\left(\int_\Gamma [\hat{n}_k(\mathbf{x}) - \hat{n}_k(\mathbf{y})]\frac{\partial \ln r}{\partial x_i} d\Gamma_x \right. \\ & + \hat{n}_k(\mathbf{y})\int_\Gamma [\hat{t}_i(\mathbf{x}) - \hat{t}_i(\mathbf{y})]\frac{\partial \ln r}{\partial \hat{\mathbf{t}}} d\Gamma_x \\ & \left.\left. + \hat{n}_k(\mathbf{y})\int_\Gamma [\hat{n}_i(\mathbf{x}) - \hat{n}_i(\mathbf{y})]\frac{\partial \ln r}{\partial \hat{\mathbf{n}}} d\Gamma_x\right)\right\}, \quad \mathbf{y} \in \Gamma\end{aligned} \tag{2}$$

For the internal point $\boldsymbol{y}$, the integral equations can be written as

$$u_i(\mathbf{y}) = \int_\Gamma \phi_k(\mathbf{x}) u^*_{ik}(\mathbf{y},\mathbf{x}) d\Gamma, \quad \mathbf{y} \in \hat{\Omega} \tag{3}$$

$$\nabla u_i(\mathbf{y}) = \int_\Gamma \phi_k(\mathbf{x}) \nabla u^*_{ik}(\mathbf{y},\mathbf{x}) d\Gamma, \quad \mathbf{y} \in \hat{\Omega} \tag{4}$$

In Eqs. (1)–(4), i, $k=1$, 2; $k_0=1/4\pi(1-\nu)$; G is the shear modulus; $\phi_k(\boldsymbol{x})$ is the density function to be determined; $u^*_{ik}(\mathbf{y},\mathbf{x})$ denotes the Kelvin fundamental solution. For interior problems, $\hat{\Omega}=\Omega$, $\hat{S}=1$, $\hat{\mathbf{t}}(\mathbf{x})$ and $\hat{\mathbf{n}}(\mathbf{x})$ are the unit tangent and outward normal vectors of Γ to domain Ω at point x, respectively. For exterior problems, $\hat{\Omega}=\Omega^c$, $\hat{S}=0$, $\hat{\mathbf{t}}(\mathbf{x})$ and $\hat{\mathbf{n}}(\mathbf{x})$ are the unit tangent and outward normal vectors of Γ to domain Ω^c at point $\boldsymbol{x}$, respectively.

The Gaussian quadrature is directly used to calculate the density function in the discretized Eqs. (1) and (2) in the CBEM. However, if the domain of a considered problem is thin, some boundaries will be very close to each other. Thus, the distance r between some boundary nodes and integral elements probably approaches zero. This would cause nearly singular integrals in Eqs. (1) and (2), and the density functions cannot be calculated accurately by Gauss quadrature, needless to say, to calculate the physical quantities at interior points. Moreover, almost all the interior points of thin bodies are very close to the integral elements. Thus, there also exist nearly singular integrals in Eqs. (3) and (4).

The above-mentioned nearly singular integrals can be expressed as the following generalized integrals:

$$\begin{cases} I_1 = \int_\Gamma \psi(\mathbf{x}) \ln r^2 \, d\Gamma \\ I_2 = \int_\Gamma \psi(\mathbf{x}) \dfrac{1}{r^{2\alpha}} \, d\Gamma \end{cases} \tag{5}$$

where $\alpha > 0$, $\psi(\boldsymbol{x})$ is a well-behaved function including the Jacobian, the shape functions and, ones which arise from taking the derivative of the integral kernels.

Note that for most of existing methods the geometry of the boundary element of Eq. (5) is often depicted by using linear shape functions. However, the linear element is not an ideal one as it cannot approximate with sufficient accuracy for the geometry of curvilinear boundaries. For this reason, it is recommended to use higher order elements—usually of second order in most applications. As shown in Ref. [17], if isoparametric quadratic boundary elements are employed, the distance square r^2 between the field point $\boldsymbol{y}$ and the source point $\boldsymbol{x}(\xi)$ can be expressed as follows:

$$r^2(\xi) = (x_k - y_k)(x_k - y_k) = (\xi - \eta)^2 g(\xi) + d^2 \tag{6}$$

Please cite this article as: Zhang Y-M, et al. Boundary element analysis of 2D thin walled structures with high-order geometry elements using transformation. Eng Anal Bound Elem (2010), doi:10.1016/j.enganabound.2010.07.008

where $d^2=(x_k(\eta)-y_k)(x_k(\eta)-y_k)$,

$$g(\xi)=\frac{1}{4}(x_k^1-2x_k^3+x_k^2)(x_k^1-2x_k^3+x_k^2)(\xi+\eta)^2 + \frac{1}{2}(x_k^1-2x_k^3+x_k^2)(x_k^2-x_k^1)(\xi+\eta) + h^2+(x_k^1-2x_k^3+x_k^2)(x_k(\eta)-y_k),$$

where $h=\frac{1}{2}\sqrt{(x_k^2-x_k^1)(x_k^2-x_k^1)}$.

With the aid of Eq. (6), the nearly singular integrals in Eq. (5) can be summarized to the following forms:

$$\begin{cases} I_1=\int_0^a f(x)\ln[x^2g(x)+d^2]dx \\ I_2=\int_0^a \dfrac{f(x)}{[x^2g(x)+d^2]^\alpha}\,dx \end{cases} \tag{7}$$

where $f(\cdot)$ is a regular function; a is a constant with respect to η.

It is obvious that the above integrals would present various orders of near singularity if d is very small. The key to achieving high accuracy is to find an algorithm to calculate these integrals accurately for a small value of d.

Introducing the following variable transformation [17,18]

$$x=d(e^{k(1+t)}-1),\quad k=\ln(1+a/d)/2 \tag{8}$$

which maps $x(o, a)$ to $t(-1,1)$. Substituting (8) into (7), then Eq. (7) can be rewritten as

$$\begin{cases} I_1=dk\int_{-1}^1 f(t)\ln[(e^{k(1+t)}-1)^2g(t)+1]e^{k(1+t)}\,dt+dk\int_{-1}^1 f(t)\ln d^2 e^{k(1+t)}\,dt \\ I_2=kd^{1-2\alpha}\int_{-1}^1 \dfrac{f(t)e^{k(1+t)}}{[(e^{k(1+t)}-1)^2g(t)+1]^\alpha}\,dt \end{cases} \tag{9}$$

By following the procedures described above, the near singularity of the boundary integrals has been fully regularized. The final integral formulations over parabolic elements are obtained as shown in Eq. (9), which can be computed straightforward by using the standard Gaussian quadrature.

3. Numerical verification

To verity the BEM formulation developed for thin structural problems, two simple test problems are studied in which BEM solutions are compared with the exact solutions.

Example 1. A thin-walled cylinder subjected to a uniform internal pressure $p=1$ is considered, as shown in Fig. 1. The outer and inner radii of the cylinder are a and b, respectively, with $a=10$. The elastic shear modulus is $G=807692.3$ N/cm^2 and the Poisson's ratio is $\nu=0.3$. The entire boundary is discretized by 60 discontinuous isoparametric quadratic elements.

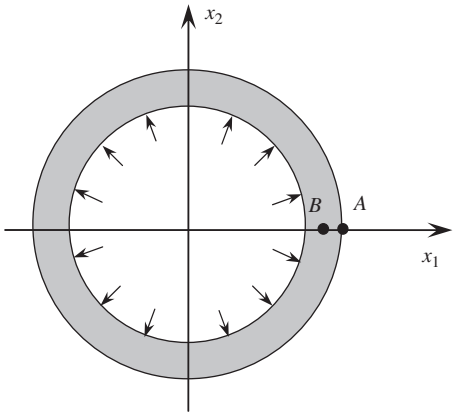

Fig. 1. A thin-walled cylinder subjected to uniform internal pressure.

In this example, $\delta=(a-b)/a$ is defined as the thickness-to-length ratio of thin-walled structures [22]. For different thickness-to-length ratios, the results of the unknown stresses at the boundary node $A(a,\ 0)$ are shown in Figs. 2 and 3. The results of the stresses and its relative error (%) at interior point $B((a+b)/2, 0)$ are listed in Tables 1 and 2. For $\delta=1.0\text{E}-6$, the stress results calculated by using the present method are listed in Tables 3 and 4.

We can observe in Fig. 2 that the radial stress σ_r at boundary node A can be accurately calculated by using the present method even when δ decreases to 1E−06. Fig. 3 illustrates that the results

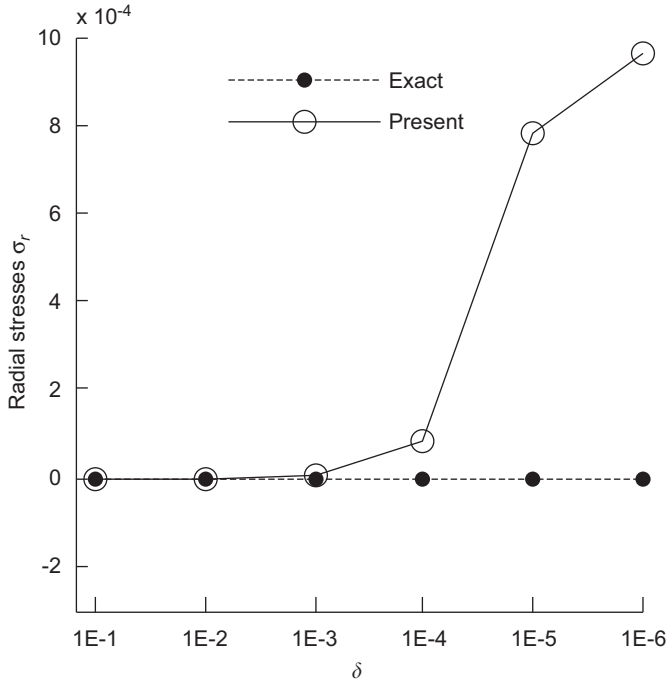

Fig. 2. Radial stresses σ_r at the boundary node A.

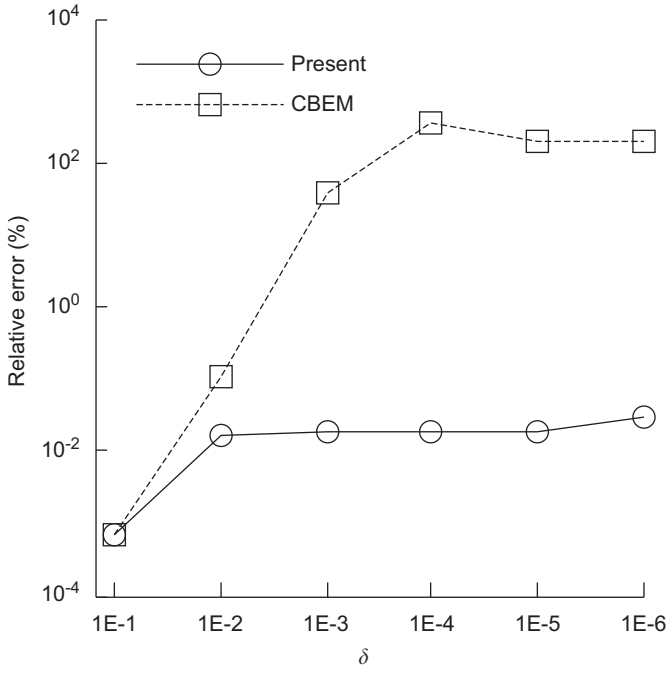

Fig. 3. Relative errors (%) of the tangential stresses σ_θ at the boundary node A.

Please cite this article as: Zhang Y-M, et al. Boundary element analysis of 2D thin walled structures with high-order geometry elements using transformation. Eng Anal Bound Elem (2010), doi:10.1016/j.enganabound.2010.07.008

Table 1
Radial stress σ_r at the interior point B.

δ	Exact	CBEM	Relative error (%)	Present	Relative error (%)
1.0E−1	−0.4605628E+00	−0.4605654E+00	−0.5639465E−03	−0.4605535E+00	0.2002811E−02
1.0E−2	−0.4962312E+00	0.1628417E+02	0.3381570E+04	−0.4962627E+00	−0.6353770E−02
1.0E−3	−0.4996248E+00	−0.3211114E+02	−0.6327051E+04	−0.4996301E+00	−0.1048724E−02
1.0E−4	−0.4999625E+00	0.1512744E+03	0.3035715E+05	−0.4999631E+00	−0.1128103E−03
1.0E−5	−0.4999962E+00	0.9089221E+02	0.1827858E+05	−0.4999964E+00	−0.3605676E−04
1.0E−6	−0.4999996E+00	0.8744101E+02	0.1758822E+05	−0.4997179E+00	0.5633904E−01

Table 2
Tangential stress σ_θ at the interior point B.

δ	Exact	CBEM	Relative error (%)	Present	Relative error (%)
1.0E−1	0.8986879E+01	0.8986873E+01	0.5684806E−04	0.8986998E+01	−0.1324860E−02
1.0E−2	0.9899874E+02	0.9137400E+02	0.7701863E+01	0.9898402E+02	0.1487651E−01
1.0E−3	0.9989999E+03	0.9317472E+03	0.6732000E+01	0.9988080E+03	0.1920986E−01
1.0E−4	0.9999000E+04	−0.4040860E+04	0.1404126E+03	0.9997082E+04	0.1918569E−01
1.0E−5	0.9999900E+05	−0.2429923E+04	0.1024299E+03	0.9997990E+05	0.1909961E−01
1.0E−6	0.9999990E+06	−0.2338491E+04	0.1002338E+03	0.9997090E+06	0.2899701E−01

Table 3
Radial stress σ_r at interior points on the line $x_2=0$ ($\delta=1.0E-6$).

x_1	Exact	CBEM	Relative error (%)	Present	Relative error (%)
9.999991	−0.8999999E+00	0.8743318E+02	0.9814799E+04	−0.9012839E+00	−0.1426687E+00
9.999992	−0.7999998E+00	0.8743514E+02	0.1102940E+05	−0.8005229E+00	−0.6538819E−01
9.999993	−0.6999997E+00	0.8743710E+02	0.1259102E+05	−0.6998743E+00	0.1791863E−01
9.999994	−0.5999996E+00	0.8743906E+02	0.1467318E+05	−0.5996231E+00	0.6275614E−01
9.999996	−0.3999996E+00	0.8744297E+02	0.2196076E+05	−0.3998028E+00	0.4920305E−01
9.999997	−0.2999997E+00	0.8744493E+02	0.2924834E+05	−0.2997886E+00	0.7037746E−01
9.999998	−0.1999998E+00	0.8744688E+02	0.4382349E+05	−0.1999138E+00	0.4299207E−01
9.999999	−0.9999986E−01	0.8744884E+02	0.8754896E+05	−0.9991639E−01	0.8347362E−01

Table 4
Tangential stress σ_θ at interior points on the line $x_2=0$ ($\delta=1.0E-6$).

x_1	Exact	CBEM	Relative error (%)	Present	Relative error (%)
9.999991	0.9999994E+06	−0.2338528E+04	0.1002339E+03	0.9997105E+06	0.2888914E−01
9.999992	0.9999993E+06	−0.2338519E+04	0.1002339E+03	0.9997101E+06	0.2891611E−01
9.999993	0.9999992E+06	−0.2338510E+04	0.1002339E+03	0.9997098E+06	0.2894310E−01
9.999994	0.9999991E+06	−0.2338500E+04	0.1002339E+03	0.9997094E+06	0.2897006E−01
9.999996	0.9999989E+06	−0.2338481E+04	0.1002338E+03	0.9997087E+06	0.2902395E−01
9.999997	0.9999988E+06	−0.2338472E+04	0.1002338E+03	0.9997083E+06	0.2905089E−01
9.999998	0.9999987E+06	−0.2338462E+04	0.1002338E+03	0.9997079E+06	0.2907783E−01
9.999999	0.9999986E+06	−0.2338453E+04	0.1002338E+03	0.9997076E+06	0.2910478E−01

of tangent stress σ_θ calculated by using CBEM become less satisfactory when δ less than 1E−02. In contrast, the results calculated by using the proposed method are very consistent with the exact solutions with the largest relative error less than 0.05% even when δ as small as 1E−06.

Tables 1 and 2 show that the CBEM can only be available to calculate the acceptable radial stress and tangent stress at the interior point B for δ down to 1E−01, the results are out of true with further decrease of δ. Nevertheless, the results obtained by using the present method are excellently consistent with the analytical solutions even when δ equals 1E−06.

Tables 3 and 4 present the results of radial stress and tangent stress at eight different interior points with δ equals 1E−06, which further demonstrate the effectiveness of the present method. In addition, the convergence curves of computed stresses at interior points B are shown in Fig. 4, from which we can observe that the convergence speeds are still fast even when δ reached 1E−06. In Fig. 4, only the errors of the present method are given, since the errors of the CBEM are relatively too large.

Example 2. As shown in Fig. 5, a thin coating with nonuniform thickness on a shaft is considered. Both the shaft and coating profiles remain circular, but their centers are misaligned (b) compared to the uniform thickness case (a), producing some normalized eccentricity $\delta=x_c/(r_b-r_a)$, where x_c is the center offset. The coating and shaft have outer radii r_b and r_a, respectively, with their center of curvature located at the point $o(0,0)$. In this example, the coated system is loaded by a uniform pressure p, and the shaft is considered to be rigid when compared to the coating, so the boundary conditions are $u_x=u_y=0$ for all nodes at the shaft/coating interface. There are totally 16 discontinuous isoparametric quadratic elements divided along

Please cite this article as: Zhang Y-M, et al. Boundary element analysis of 2D thin walled structures with high-order geometry elements using transformation. Eng Anal Bound Elem (2010), doi:10.1016/j.enganabound.2010.07.008

the shaft and coating surfaces, regardless of the thickness of the structure. The elastic shear modulus is $G=8.0\times10^{10}$ Pa and Poisson's ratio is $\nu=0.2$.

While no analytical solution exists for $\delta\neq0$ case, the asymptotic behavior of the solution as $\delta\to0$ can be checked to verify the formulation. In this example, shaft radius is held constant at 0.1 and coating outer radius is also constant at 0.11; the eccentricity has been systematically varied over the entire range $0\leq\delta<1$.

In 1998, Luo et al. [21] have handled this coating system, and the radial stress σ_r at boundary node C has been obtained by using the BEM. However, in their work only boundary unknown radial stresses σ_r are computed. The boundary unknown tangential stresses σ_θ and physical quantities at interior points need further investigation. In this paper, both boundary unknowns and physical quantities at interior points over different δ are given.

Fig. 6 shows the tangential stress prediction σ_θ at boundary node C (Note that the highest normalized eccentricity solved is $\delta=0.999999$). Fig. 7 shows the normalized radial stress σ_r at boundary node C, and the results obtained by using Ref. [21] and the FEM are also given to make comparison. Note first that the asymptotic behavior of the BEM solution, which approaches the analytical value of the sample problem as $\delta\to0$ (case a). Also notice that the same stress value at point C approaches the applied pressure p as $\delta\to1$, which is consistent with the physical interpretation. The FEM solution, however, demonstrates a very

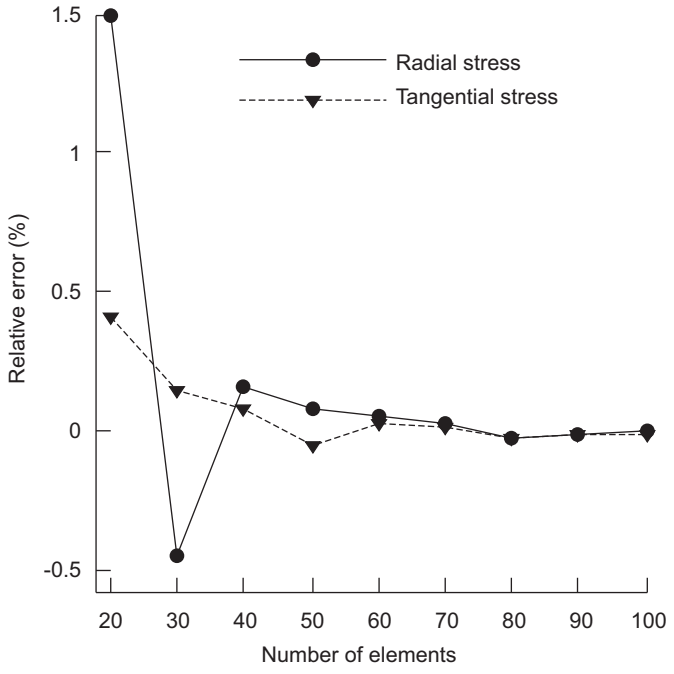

Fig. 4. Convergence curves of the stresses at the interior point B with $\delta=1.0\text{E}-6$.

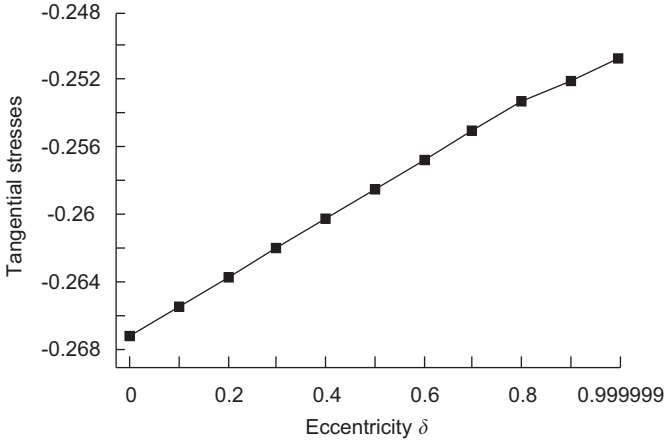

Fig. 6. Tangential stress at the boundary node C.

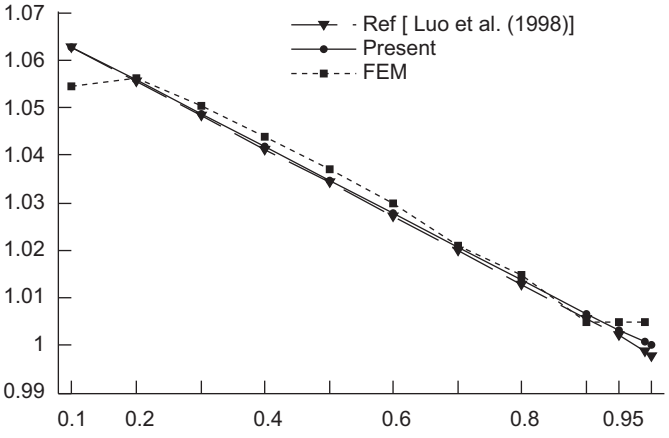

Fig. 7. Radial stress prediction at the boundary node C.

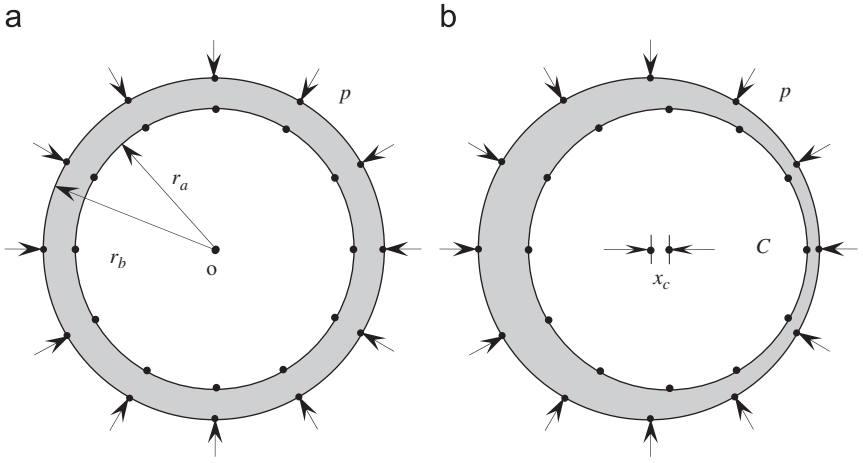

Fig. 5. A thin coating with nonuniform thickness on a shaft.

Please cite this article as: Zhang Y-M, et al. Boundary element analysis of 2D thin walled structures with high-order geometry elements using transformation. Eng Anal Bound Elem (2010), doi:10.1016/j.enganabound.2010.07.008

Table 5
Radial and tangential stress prediction for $\delta=0.999999$.

θ	Stresses at boundary nodes		Stresses at interior points	
	σ_r	σ_θ	σ_r	σ_θ
0	−0.1000000E+01	−0.2504534E+00	−0.1000000E+01	−0.2504112E+00
$\pi/6$	−0.1000000E+01	−0.2501923E+00	−0.1004975E+01	−0.2547527E+00
$\pi/4$	−0.1000000E+01	−0.2509350E+00	−0.1010772E+01	−0.2612035E+00
$\pi/3$	−0.1000000E+01	−0.2528999E+00	−0.1018067E+01	−0.2711574E+00
$\pi/2$	−0.1000000E+01	−0.2610801E+00	−0.1034176E+01	−0.3010530E+00
$2\pi/3$	−0.1000000E+01	−0.2725530E+00	−0.1047760E+01	−0.3358898E+00
$5\pi/6$	−0.1000000E+01	−0.2813670E+00	−0.1056084E+01	−0.3621889E+00
π	−0.1000000E+01	−0.2843456E+00	−0.1058817E+01	−0.3717277E+00

different behavior. While the low eccentricity cases are easily solved with the FEM with a fairly small number of elements, the solution requires significantly more effort for $\delta\to1$. Indeed, studies in Ref. [21] show that for $\delta>0.99$, the FEM solution becomes infeasible due to memory limitations.

In addition, for different angular coordinates, the radial and tangential stress prediction for $\delta=0.999999$ at the boundary nodes (r_a, θ) and at the interior points ((r_a+r_b)/2, θ) are given in Table 5.

4. Conclusion

In this paper, an efficient BEM-based technique is developed for thin structural problems occurring in 2D elasticity problems. The seemingly difficult task of evaluating the nearly singular integrals in the BIE can be dealt with accurately and efficiently by using a general non-linear transformation. Two numerical examples of elastic thin-walled structures with thickness-to-length ratios ranging from 1E−01 to 1E−06 are presented to test the proposed method. Both boundary unknown variables on the boundary and physical quantities at interior points are accurately calculated. Owing to the employment of the high-order element, only a small number of elements need to be divided along the boundary, and high accuracy can be achieved without increasing more computational efforts.

The developed method of using the BEM can be extended readily to model layered or multilayered coatings, thin films and other more realistic models. Some work along this line for thin structures is already underway.

In addition, extensive numerical experiments have indicated that the proposed method is expected more efficient, in terms of the necessary integration points and CPU-time, compared to previous transformation methods when the thickness of considered structures is less than 10^{-6}. In the follow-up work, the author and co-workers will give some comments on the previous results concerning transformations for calculating nearly singular integrals using the boundary element analysis.

Acknowledgments

The support of the National Natural Science Foundation of China (No. 10571110) and the Natural Science Foundation of Shandong Province of China (No. 2003ZX12) is gratefully acknowledged.

References

[1] Cruse TA. Boundary element analysis in computational fracture mechanics. Dordrecht, Boston. Kluwer Academic Publishers; 1988.
[2] Luo JF, Liu YJ, Berger EJ. Interfacial stress analysis for multi-coating systems using an advanced boundary element method. Computational Mechanics 2000;24(6):448–55.
[3] Brebbia CA. The boundary element method for engineers. London, New York: Pentech Press; 1978.
[4] Jun L, Beer G, Meek JL. Efficient evaluation of integrals of order 1/r 1/r2, 1/r3 using Gauss quadrature. Engineering Analysis 1985;2(3):118–23.
[5] Gao XW, Yang K, Wang J. An adaptive element subdivision technique for evaluation of various 2D singular boundary integrals. Engineering Analysis with Boundary Elements 2008;32(8):692–6.
[6] Lutz E. Exact Gaussian quadrature methods for near-singular integrals in the boundary element method. Engineering Analysis with Boundary Elements 1992;9(3):233–45.
[7] Yoon SS, Heister SD. Analytic solution for fluxes at interior points for the 2D Laplace equation. Engineering Analysis with Boundary Elements 2000;24(2):155–60.
[8] Fratantonio M, Rencis JJ. Exact boundary element integrations for two-dimensional Laplace equation. Engineering Analysis with Boundary Elements 2000;24(4):325–42.
[9] Niu ZR, Cheng CZ, Zhou HL, Hu ZJ. Analytic formulations for calculating nearly singular integrals in two-dimensional BEM. Engineering Analysis with Boundary Elements 2007;31(12):949–64.
[10] Zhou HL, Niu ZR, Cheng CZ, Guan ZW. Analytical integral algorithm in the BEM for orthotropic potential problems of thin bodies. Engineering Analysis with Boundary Elements 2007;31(9):739–48.
[11] Sladek V, Sladek J, Tanaka M. Optimal transformations of the integration variables in computation of singular integrals in BEM. International Journal for Numerical Methods in Engineering 2000;47(7):1263–83.
[12] Huang Q, Cruse TA. Some notes on singular integral techniques in boundary element analysis. International Journal for Numerical Methods in Engineering 1993;36(15):2643–59.
[13] Johnston PR, Elliott D. A sinh transformation for evaluating nearly singular boundary element integrals. International Journal for Numerical Methods in Engineering 2005;62(4):564–78.
[14] Ma H, Kamiya N. Distance transformation for the numerical evaluation of near singular boundary integrals with various kernels in boundary element method. Engineering Analysis with Boundary Elements 2002;26(4):329–39.
[15] Telles JCF. A self-adaptive co-ordinate transformation for efficient numerical evaluation of general boundary element integrals. International Journal for Numerical Methods in Engineering 1987;24(5):959–73.
[16] Nagarajan A, Mukherjee S. A mapping method for numerical evaluation of two-dimensional integrals with 1/r singularity. Computational Mechanics 1993;12(1):19–26.
[17] Zhang YM, Gu Y, Chen JT. Boundary layer effect in BEM with high order geometry elements using transformation. Computer Modeling in Engineering & Sciences 2009;45(3):227–47.
[18] Zhang YM, Sun CL. A general algorithm for the numerical evaluation of nearly singular boundary integrals in the equivalent non-singular BIEs with indirect unknowns. Journal of the Chinese Institute of Engineers 2008;31(3):437–47.
[19] Sladek V, Sladek J, Tanaka M, Nonsingular BEM. formulations for thin-walled structures and elastostatic crack problems. Acta Mechanica 1993;99(1):173–90.
[20] Liu YJ. Analysis of shell-like structures by the boundary element method based on 3-D elasticity: formulation and verification. International Journal for Numerical Methods in Engineering 1998;41(3):541–58.
[21] Luo JF, Liu YJ, Berger EJ. Analysis of two-dimensional thin structures (from micro- to nano-scales) using the boundary element method. Computational Mechanics 1998;22(5):404–12.
[22] Zhou HL, Niu ZR, Cheng CZ, Guan ZW. Analytical integral algorithm applied to boundary layer effect and thin body effect in BEM for anisotropic potential problems. Computers & Structures 2008;86(15–16):1656–71.
[23] Zhang YM, Gu Y, Chen JT. Boundary element analysis of the thermal behaviour in thin-coated cutting tools. Engineering Analysis with Boundary Elements 2010;34(9):775–84.
[24] Zhang YM, Wen WD, Wang LM, Zhao XQ. A kind of new nonsingular boundary integral equations for elastic plane problems. Chinese Journal of Theoretical and Applied Mechanics 2004;36(3):311–21.

Please cite this article as: Zhang Y-M, et al. Boundary element analysis of 2D thin walled structures with high-order geometry elements using transformation. Eng Anal Bound Elem (2010), doi:10.1016/j.enganabound.2010.07.008